








## RESEARCH ARTICLE

# Representation of Dense Shelf Water formation by global oceanic reanalyses

Rafael Afonso do Nascimento Reis,<sup>1,2</sup>  Flávio Justino,<sup>1</sup>  Luis Felipe Ferreira de Mendonça,<sup>3</sup>  Riccardo Farneti,<sup>4</sup>  Marcos Tonelli,<sup>5</sup>  Jeferson Prietsch Machado<sup>6</sup>  & Douglas da Silva Lindemann<sup>7</sup> 

<sup>1</sup>Departamento de Engenharia Agrícola, Universidade Federal de Viçosa, Viçosa, Brazil; <sup>2</sup>Departamento de Oceanografia e Ecologia, Universidade Federal do Espírito Santo, Vitória, Brazil; <sup>3</sup>Departamento de Oceanografia, Instituto de Geociências, Universidade Federal da Bahia, Salvador, Brazil; <sup>4</sup>Earth System Physics Section, International Centre for Theoretical Physics, Trieste, Italy; <sup>5</sup>Admiral Paulo Moreira Institute for Marine Studies, Arraial do Cabo, Brazil; <sup>6</sup>Instituto de Oceanografia, Universidade Federal do Rio Grande, Rio Grande, Brazil; <sup>7</sup>Departamento de Meteorologia, Universidade Federal de Pelotas, Pelotas, Brazil

## Abstract

This study evaluates the representation of Dense Shelf Water (DSW) formation in the Southern Ocean by two global oceanic reanalyses: GLORYS2v4 and ORAS5. We found that GLORYS2v4 generally represents larger areas and more consistent temporal patterns of DSW compared to ORAS5. This latter reanalysis significantly underestimates the extent and frequency of DSW formation. Although both reanalyses show good statistical agreement with the World Ocean Circulation Experiment data set, with a root mean squared error of approximately 0.7, a mean absolute percentage error of 1.16% and an  $r$  value of 0.99, ORAS5 fails to reproduce the expected sea-surface salinity trend, exhibiting a negative trend across most of the Southern Ocean. This may lead to a weak representation of the water-mass formation processes in the region, thereby affecting its ability to satisfactorily represent the Meridional Overturning Circulation and the global thermohaline circulation. These discrepancies are attributed to the nudging process used for the sea-surface temperature in the ORAS5 model. This study highlights the importance of oceanic reanalyses to validate climate modelling results, in particular in high-latitude regions, where observations are scarce and crucial for understanding global climatic changes.

## Keywords

GLORYS; ORAS5; sea surface salinity; Dense Shelf Water; nudging

## Correspondence

Rafael Afonso do Nascimento Reis,  
Departamento de Engenharia Agrícola,  
Universidade Federal de Viçosa, Sala 107,  
36570-900 Viçosa, Minas Gerais, Brasil.  
E-mail: rafael\_cgb@hotmail.com

## Abbreviations

CORA5:	Coriolis Ocean Database for Reanalysis
DSW:	Dense Shelf Water
EN4:	version 4 of the Met Office Hadley Centre EN series
ERA-Interim:	European Centre for Medium-Range Weather Forecasts Interim reanalysis
GLORYS2v4:	Mercator Ocean Global Ocean Physics Reanalysis 2, version 4
MAPE:	mean absolute percentage error
ORAS5:	European Centre for Medium-Range Weather Forecasts Ocean Reanalysis System 5
ORCA-R025:	a global ocean configuration of the NEMO-OPA ocean circulation model
RMSE:	root mean squared error
SO:	Southern Ocean (south of 30°S)
SSS:	sea-surface salinity
SST:	sea-surface temperature
WOCE:	World Ocean Circulation Experiment

To access the supplementary material, please visit the article landing page

## Introduction

Over the years, several studies have been conducted across the SO, demonstrating that processes occurring there are controlled by complex, and not fully elucidated, interactions between the ocean, atmosphere and land/sea-ice conditions (Rintoul 2018). Absorbing about 40–50% of anthropogenic CO<sub>2</sub>, the SO plays a significant part in the global carbon dioxide variability (Sabine et al. 2004; Watson & Garabato 2006; Frölicher et al. 2015).

Moreover, the SO takes up more than 70% of the heat related to anthropogenic activities (Dufour et al. 2015; Frölicher et al. 2015).

The lack of physical barriers in the SO allows for development of the Antarctic Circumpolar Current, which links oceanic basins by transporting water from one basin to another (Farneti et al. 2015). The circulation and water mass transformation in the SO are fundamental for the global oceanic circulation (Sloyan & Rintoul 2001; Sarmiento et al. 2004; Marinov et al. 2006; Marshall &

Speer 2012; Farneti et al. 2015). The ocean–atmosphere–cryosphere interactions in the SO, through surface buoyancy and wind-stress, set the magnitude and the pattern of the Meridional Overturning Circulation (Sloyan & Rintoul 2001; Lumpkin & Speer 2007; Marshall & Speer 2012; Abernathy et al. 2016; Pellichero et al. 2018; Rintoul 2018).

Part of the Meridional Overturning Circulation in the SO is the ascending branch of the deep water generated in the North Atlantic, known as North Atlantic Deep Water, which flows southward and is transformed into Upper Circumpolar Deep Water and Lower Circumpolar Deep Water (Talley et al. 2011). Upper Circumpolar Deep Water ascends to the surface and, through air–sea buoyancy fluxes, is converted into Antarctic Intermediate Water and Subantarctic Mode Water, which flow northward, submerging in the subtropical front and occupying the upper layers of oceanic gyres. This mechanism ventilates these regions (Sloyan & Rintoul 2001; Hartin et al. 2011; Farneti et al. 2015). Lower Circumpolar Deep Water emerges near the Antarctic coast and, through air–sea–ice interactions, is integrated into Antarctic Bottom Water (Gordon 2001; Marshall & Speer 2012). The ascension of water in the Meridional Overturning Circulation provides nutrients from the intermediate and deep ocean to the surface, which, according to model simulations, is responsible for three-quarters of primary production north of 30°S (Sarmiento et al. 2004; Marinov et al. 2006).

The formation of these water masses and how water is transported in the SO, and the nature of how ocean–atmosphere–cryosphere interactions modulate these processes, are key points for understanding the distribution of heat, CO<sub>2</sub> and oxygen throughout the global ocean (Banks & Gregory 2006; Talley et al. 2011; Khatiwala et al. 2013; Marshall et al. 2015; Yamamoto et al. 2015). Although we know that the SO is important, it is poorly sampled and accurate modelling results are scarce (Silvano 2020). In recent years, many studies have evaluated ocean models and reanalysis, with the aim of producing satisfactory representations of the complex processes that occur in the SO (Justino et al. 2011; Bracegirdle et al. 2013; Sallée et al. 2013; Downes et al. 2015; Farneti et al. 2015; Justino et al. 2015; Wang & Dommenget 2015; Schneider & Reusch 2016; Wang et al. 2018; Almeida et al. 2021). However, the lack of in situ observations means that several questions remain regarding the atmospheric influence on surface density, which subsequently modifies the characteristics and magnitude of water mass formation. For example, Antarctic Bottom Water sinks to the abyssal layer of the global ocean (Orsi et al. 1999), occupying between 30 and 40% of the total global ocean volume (Johnson 2008). Its formation is important for heat and CO<sub>2</sub> transport from the surface to the ocean bottom (Sigman & Boyle 2000), and it is also part of the Meridional Overturning Circulation (Orsi et al. 1999; Johnson 2008; Marshall & Speck 2012).

One important component of Antarctic Bottom Water is the DSW, which is formed near the Antarctic Peninsula, where there is a direct contact between the relatively warm ocean surface and colder air from the Antarctic continent. The resulting massive ocean heat loss generates high rates of sea-ice production (Tamura et al. 2008), which—through brine rejection—substantially increases the density of coastal waters over the Antarctic Continental Shelf. How DSW is formed is an ideal test case to show how the representation of density surface layers can have an impact on how different reanalyses products simulate SO water masses.

This formation process occurs in very few locations: the Weddell Sea (Foster & Carmack 1976; Gordon et al. 1993; Foldvik et al. 2004; Moorman et al. 2020), the Ross Sea (Jacobs et al. 1970; Gordon et al. 2004; Gordon et al. 2009; Moorman et al. 2020), the Adélie Coast (Foster 1995; Rintoul 1998; Williams et al. 2010; Moorman et al. 2020) and Prydz Bay (Ohshima et al. 2013; Williams et al. 2016). The Weddell Sea was chosen for this study because, out of the three known locations, it is responsible for 66% of the Antarctic Bottom Water formation (Talley et al. 2011).

Here we to analyse the fidelity of GLORYS2v4 (Ferry et al. 2010) and ORAS5 (Zuo et al. 2019) reanalyses in representing DSW formation in the SO. These reanalyses were chosen because both use the same models but with some differences in the simulation of the SST that might generate some discrepancies. An additional factor for their selection was the lack of their assessment in the SO: a better understanding of their representation of the SO could support future studies in this region. To this end, we compare reanalysis data with conductivity–temperature–depth data from the WOCE data set across the SO to assess the effectiveness of the data assimilation products.

## Methodology

### *Oceanographic reanalyses and in situ data*

In this study we use two global oceanic reanalyses based on monthly averaged data: GLORYS2v4 and ORAS5 (Table 1). Although GLORYS2v4 and ORAS5 essentially employ the same assimilation method and use ORCA-R025 as the global configuration (Barnier et al. 2006), ORAS5 differs from GLORYS2v4 because its SST is constrained by climatology nudging, which may cause divergence between the two reanalyses.

We obtained the in situ data from WOCE (Boyer et al. 2019) for the 1993–2014 period, an interval that overlaps with both reanalyses time ranges. WOCE data were chosen because our focus was to investigate isopycnal layers in the water columns, through the neutral density computation, and a database that has both potential temperature and salinity variables is required.

**Table 1** Features of the reanalysis GLORYS2v4 and ORAS5 products.

Features	GLORYS2v4	ORAS5
Model	NEMO 3.1 + LIM2	NEMO 3.4.1 + LIM2
Horizontal resolution	1/4° by 1/4°	25 km in the tropics; 9 km in the Arctic
Vertical levels	75	75
Atmospheric forcing	ERA-Interim	ERA-Interim
Temperature/salinity observational data	EN4, CORA <sup>a</sup>	EN4, CTDs <sup>b</sup> , buoys; Argo floats
SST data	AVHRR & AMSR-E <sup>c</sup>	HadISSTv2 & OSTIA <sup>d</sup>
Data range	1993–2016	1979–present

<sup>a</sup>Coriolis Ocean Dataset for Reanalysis. <sup>b</sup>Conductivity–temperature–density instruments. <sup>c</sup>Advanced Very High Resolution Radiometer and Advanced Microwave Scanning Radiometer for EOS. <sup>d</sup>The Met Office Hadley Centre’s sea ice and SST data set and Operational Sea Surface Temperature and Sea Ice Analysis.

Evaporation-minus-precipitation data and heat flux were taken from the ERA-Interim (Uppala et al. 2008; Dee et al. 2011) because Nicolas & Bromwich (2011) showed that out of six atmospheric reanalyses, this one shows the best representation of evaporation-minus-precipitation patterns in the SO. It is also the atmospheric forcing for GLORYS2v4 and ORAS5.

### Neutral density

A function of salinity, temperature, pressure, latitude and longitude (Eqn. 1), neutral density ( $\gamma^n$ ) determines the isopycnal surfaces in the water column and across different bodies of water (Jackett & McDougall 1997).

$$\nabla\gamma^n = b\rho(\beta\nabla S - \alpha\nabla\theta), \quad (1)$$

where  $b$  is an integrating factor,  $\rho$  is the density of seawater,  $\beta$  is the coefficient of saline contraction,  $\alpha$  is the coefficient of thermal expansion,  $S$  is salinity and  $\theta$  is the potential temperature.

It is important to note that although there is practically no difference between neutral density and potential density at the surface, surface neutral density ( $\gamma_s^n$ ) was chosen to maintain consistency with previous works, such as those of Williams et al. (2016) and Akhondas et al. (2021).

### DSW

DSW has been defined as waters with a temperature ranging from -1.9 to -1.8 °C and salinity higher than 34.5 (Foster & Carmack 1976; Baines & Condie 1998). DSW is more commonly defined as having  $\gamma^n$  value higher than 28.27. This  $\gamma^n$  value can be also associated with the AABW (Gordon 2001; Rintoul 2007; Marshall & Speer 2012; Azaneu et al. 2013). Here, DSW and AABW are assumed to be found at the same  $\gamma^n$ , as previously assumed by Williams et al. (2016).

Although DSW can be formed in the subsurface through mixing, we restricted our analysis to the formation of the water mass at the surface, through interaction

with sea ice. We also use a point in the Weddell Sea in each of the reanalyses where there is the highest number of months with the presence of DSW.

### Statistical analysis

The BIAS is a systematic difference between the model and the true value, in this case the WOCE data value:

$$\text{BIAS} = \hat{Y}_i - Y_i, \quad (2)$$

where  $\hat{Y}_i$  is the predicted value and  $Y_i$  is the true value for the  $i$ -th observation.

MAPE is another metric used to evaluate the accuracy of a predictive model. It measures the average percentage difference between predicted and true values:

$$\text{MAPE} = \frac{1}{n} \sum_{i=1}^n \frac{|Y_i - \hat{Y}_i|}{Y_i} \times 100, \quad (3)$$

where  $n$  is the number of observations,  $Y_i$  is the true value and  $\hat{Y}_i$  is the predicted value for the  $i$ -th observation.

RMSE is a measure of the average magnitude of the errors between predicted values and observed or true values in a model. It is a common metric used to assess the accuracy of a predictive model. The equation for RMSE is as follows:

$$\text{RMSE} = \sqrt{\sum_{i=1}^n \frac{(Y_i - \hat{Y}_i)^2}{n}}, \quad (4)$$

where  $n$  is the number of observations,  $Y_i$  is the true value and  $\hat{Y}_i$  is the predicted value for the  $i$ -th observation.

### Results

GLORYS2v4 and ORAS represent regions previously recognized as DSW source regions (Fig. 1): Weddell Sea (Foster & Carmack 1976; Gordon et al. 1993; Moorman et al. 2020), Ross Sea (Jacobs et al. 1970; Gordon et al. 2004;

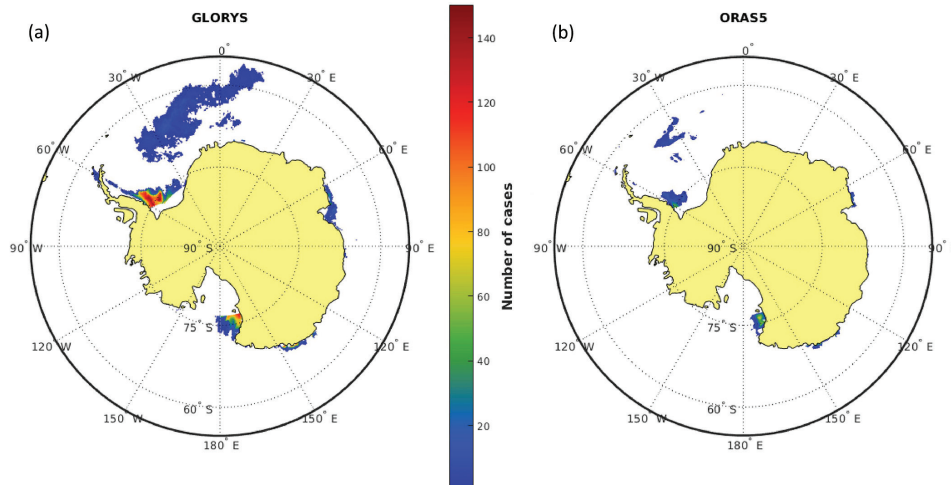


**Fig. 1** Regions with formation of Dense Shelf Water (DSW) and number of months during which DSW is at the surface layers, according to (a) GLORYS2v4 and (b) ORAS5.

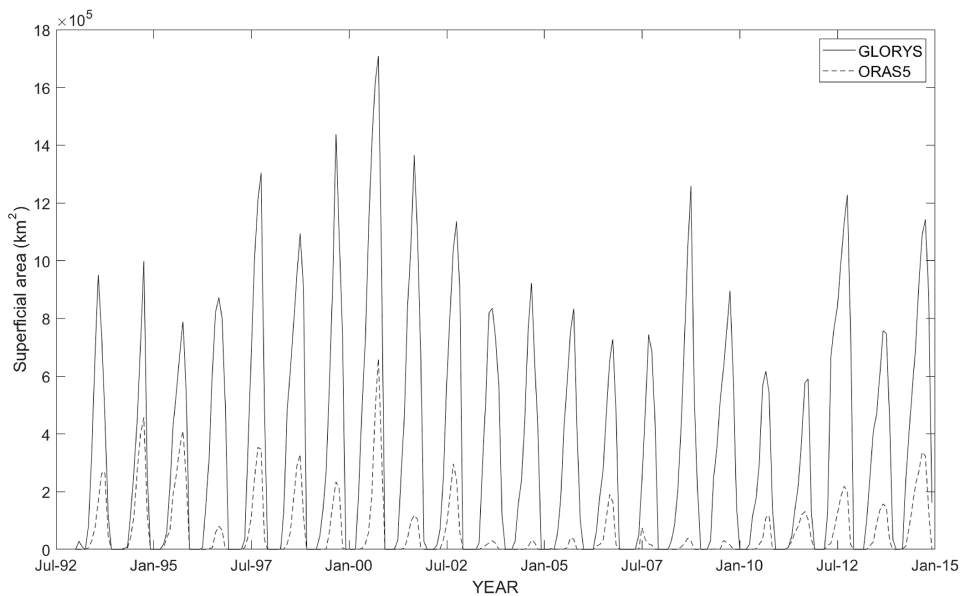


**Fig. 2** Surface area with Dense Shelf Water (DSW) in the SO for the two reanalyses used in this study.

Gordon et al. 2009; Moorman et al. 2020), Adélie Coast (Foster 1995; Williams et al. 2010; Moorman et al. 2020) and Prydz Bay (Ohshima et al. 2013; Moorman et al. 2020). ORAS5 presents smaller DSW areas, mainly along the Adélie Coast and in Prydz Bay, and fewer months with surface DSW.

The total area with surface DSW shows a direct impact of the salinity differences between the reanalyses (Fig. 2). GLORYS2v4 has a period of surface dense water source starting in April and ending in November. ORAS5 presents the same generation period, except during 2007–2010, where it presents source regions between June and October, with total areas up to 106 km<sup>2</sup> smaller than GLORYS2v4.

To better understand the differences between the two reanalyses, and to investigate the reason why ORAS5 presents much lower values compared to GLORYS2v4, we took two representative points in the region—where both data sets have the largest number of months with the presence of source regions in the Weddell Sea—and we analysed these two points surface features (Figs. 3, 4, 5; Table 2). ORAS5 has an average temperature that is 0.15°C lower than GLORYS2v4 throughout the analysed period (Fig. 2). The seasonal variability of both is very similar and approximately 0.2°C. Both reanalyses show very similar negative DSW temperature

trends, but ORAS5 no longer shows DSW production in the Weddell Sea after 2009.

As seen in the temperature profiles (Fig. 3), the formation of DSW is not always linked to the decrease of temperature. In fact, in some cases it coincides with the year's peak temperature, but the same is not true for salinity.

In the salinity time series (Fig. 4), it is noticeable that DSW formation only occurs when salinity increases above 34.55, which might explain the smaller DSW formation shown by ORAS5. GLORYS2v4 has a positive trend in salinity and values that reach 34.67, where DSW

is so dense that it can form Antarctic Bottom Water on its own (Williams et al. 2016) in most of the months between 1998 and 2003, as well as in 2006, 2009 and 2014. ORAS5, on the other hand, has a negative trend (Table 2) and shows this dense variety of DSW during fewer months (three or less) in the years of 1994, 1995, 1997, 1998, 2000 and 2002.

Focusing on DSW formation region in the Weddell Sea, we can see more clearly that GLORYS2v4 shows an increase in salinity for the entire region where DSW is formed, and that ORAS5 shows a dipole in the region: a

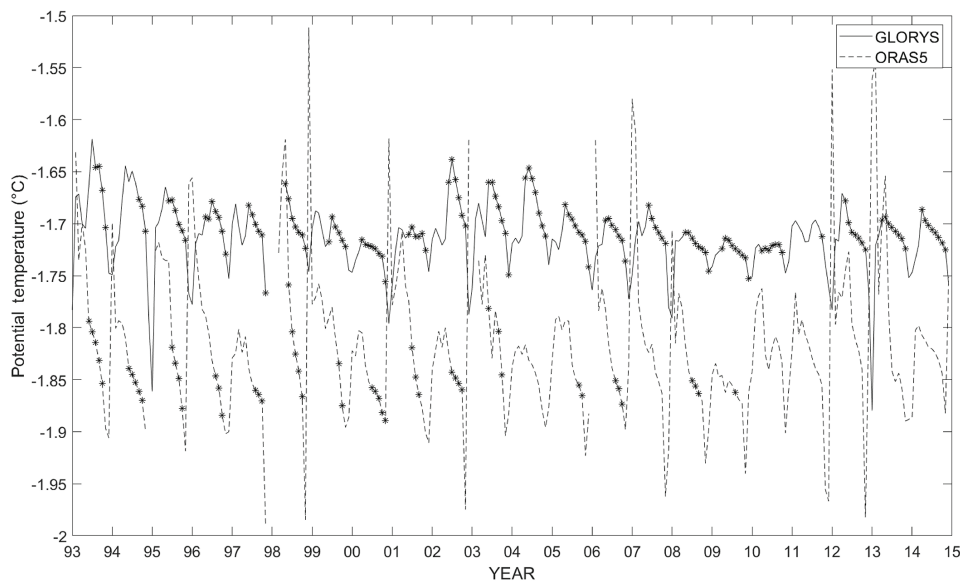


**Fig. 3** Potential temperature (°C) for the point with maximum formation of Dense Shelf Water (DSW). Values marked with asterisks represent DSW.

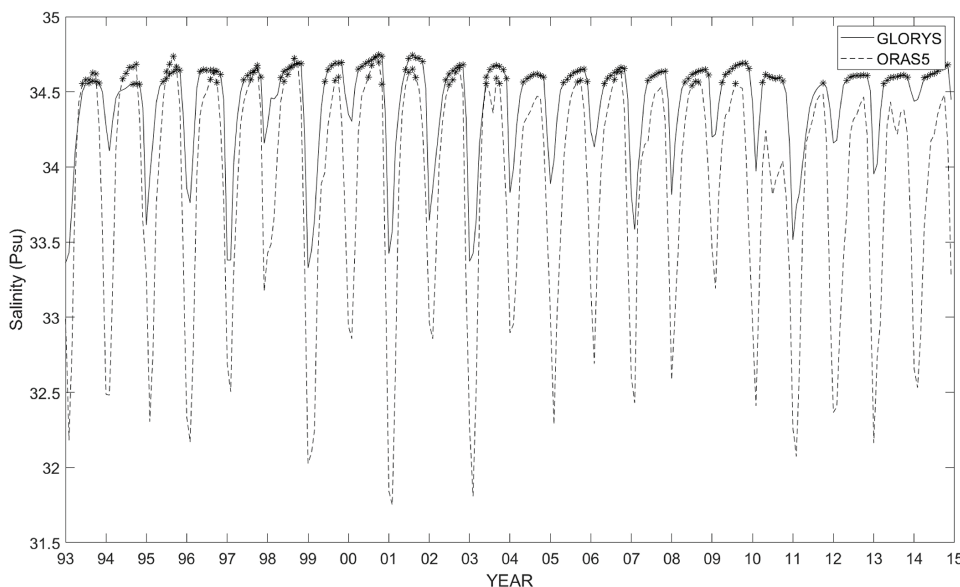


**Fig. 4** Salinity for the point with maximum formation of Dense Shelf Water (DSW). Values marked with asterisks represent DSW.



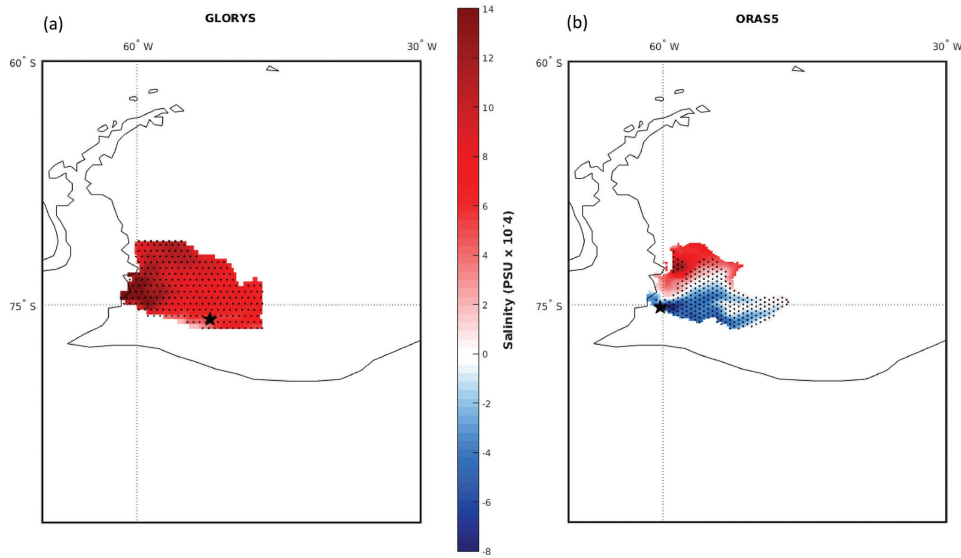


**Fig. 5** Salinity trends for the areas of Dense Shelf Water (DSW) formation in the Weddell Sea; dots indicate statistically significant trends according to (a) GLORYS2v4 and (b) ORAS5. The star marks the point with the maximum DSW formation.

**Table 2** Annual trend of temperature and salinity for the Dense Shelf Water (DSW) at the point of maximum formation (Fig. 5). All the trends are significant at the 95% confidence level.

Model	Temperature (°C/yr)	Salinity (PSU/yr)
GLORYS2v4	-0.0011	0.007
ORAS5	-0.0012	-0.0065

decrease of salinity southward and an increase in areas northward. Areas with a positive trend have nearly no statistical significance and the areas with negative trends are the areas with maximum DSW formation. Even though it may be argued that ORAS5 does not present more DSW after 2009 because the chosen point lies in a region with negative trends (Fig. 5b), in fact, ORAS5 shows that the Weddell Sea as a whole does not present any formation of DSW after 2009.

The temperature–salinity diagram of the DSW formation region in the Weddell Sea (Fig. 6) corroborates the data sampled by the regions of maximum DSW formation. Although ORAS5 shows lower temperatures at several points, it still has much less DSW than GLORYS2v4. This is evident from the salinity limit line of approximately 34.55 that delimits DSW. This underscores the importance of representing salinity in the SO, especially in regions where salinity is the main factor in the formation of water masses.

Surface salinity trends in the Weddell Sea are similar for both reanalyses during the austral summer (Fig. 7). However, trends during the winter months show great differences. GLORYS2v4 shows warming throughout

almost all of the Weddell Sea and ORAS5 shows a dipole, with negative/positive trends in the south/north. The winter months start to differ between the reanalyses because of the impacts of the SST nudging process of ORAS5. The nudging generates a misinterpretation at high-latitudes and at sea-ice edges, generating spurious oceanic convection and anomalously dense waters (Dunstone & Smith 2010; Servonnat et al. 2014).

Previous studies have pointed out how the increase in salinity by brine rejection from sea-ice formation in the Antarctic shelves increases seawater density in the region (Pellichero et al. 2018; Moorman et al. 2020). Despite showing an increase in sea-ice thickness greater than GLORYS2v4 for most of the Weddell Sea (Fig. 8), ORAS5 still presents a negative salinity trend in winter months across the southern portion of the Weddell Sea. This leads us to the conclusion that a process other than ice formation controls salinity variations in the region.

### Sea-surface salinity in the SO

The SSS statistics analyses (BIAS, RMSE, MAPE and  $r$ ) calculated for the reanalyses and for WOCE suggest that both reanalyses represent the SO well, with a salinity RMSE of approximately 0.7 for both, a MAPE inferior to 1.2% and a  $r$  value of 0.99 with 95% confidence. Differences in salinity between the reanalyses and WOCE show greater error in the 1990s (Fig. 9b, d). This is possibly related to the fact that although the era of satellite observations had already begun, it was only in the late 1990s and early 2000s that the high-latitude regions of

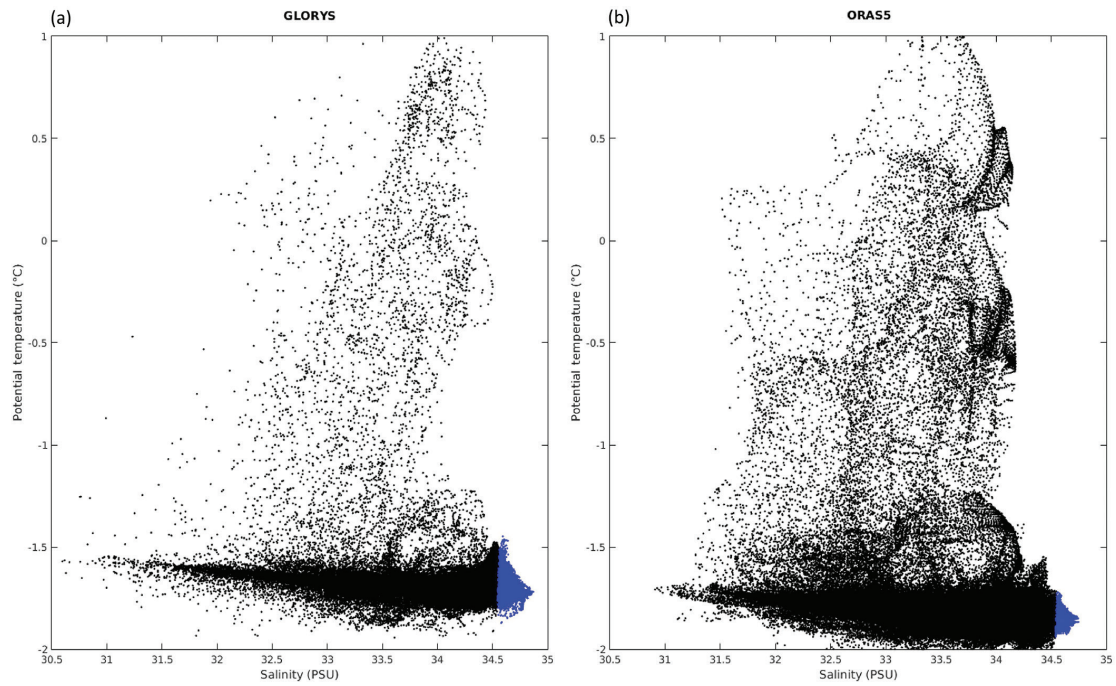


**Fig. 6** Temperature–salinity diagram of the surface region of Dense Shelf Water (DSW) formation in the Weddell Sea, according to (a) GLORYS2v4 and (b) ORAS5. Blue points are DSW. ORAS5 has a higher number of sampled points because of its higher resolution.

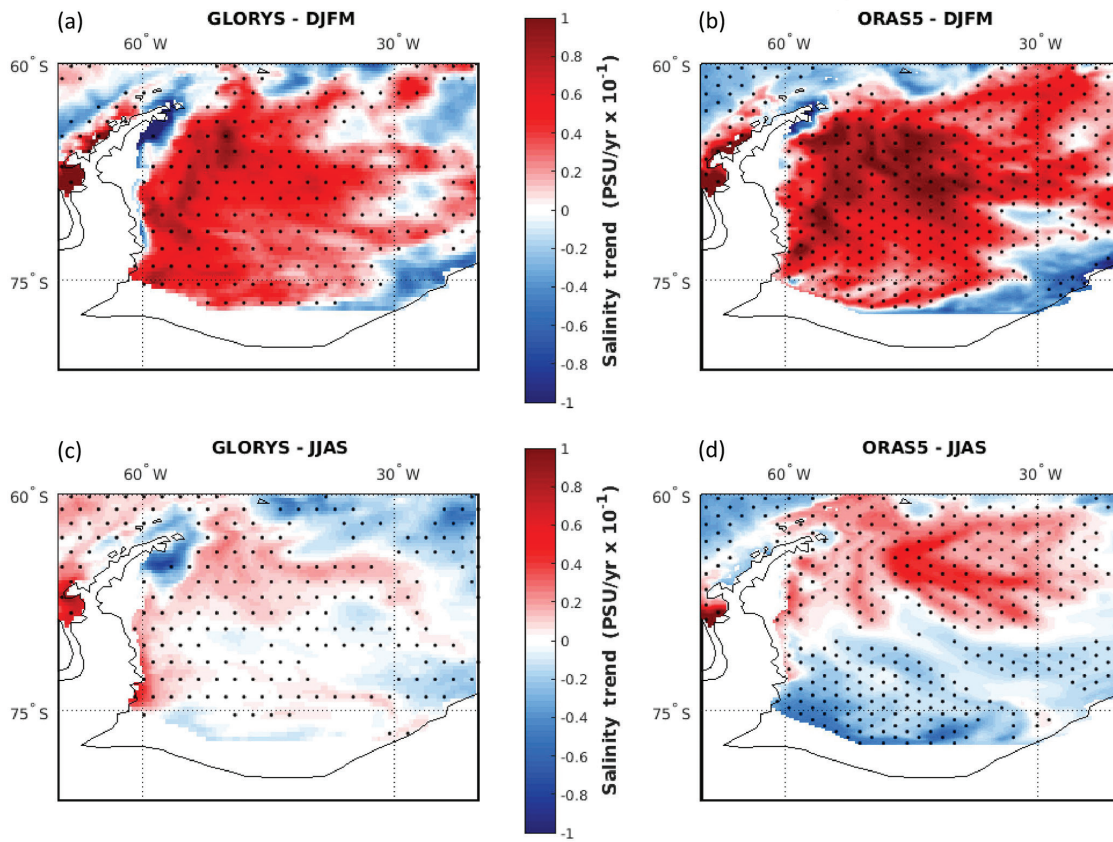


**Fig. 7** Salinity trends in the Weddell Sea for (a, b) austral winter and (c, d) summer, according to (a, c) GLORYS2v4 and (b, d) ORAS5.

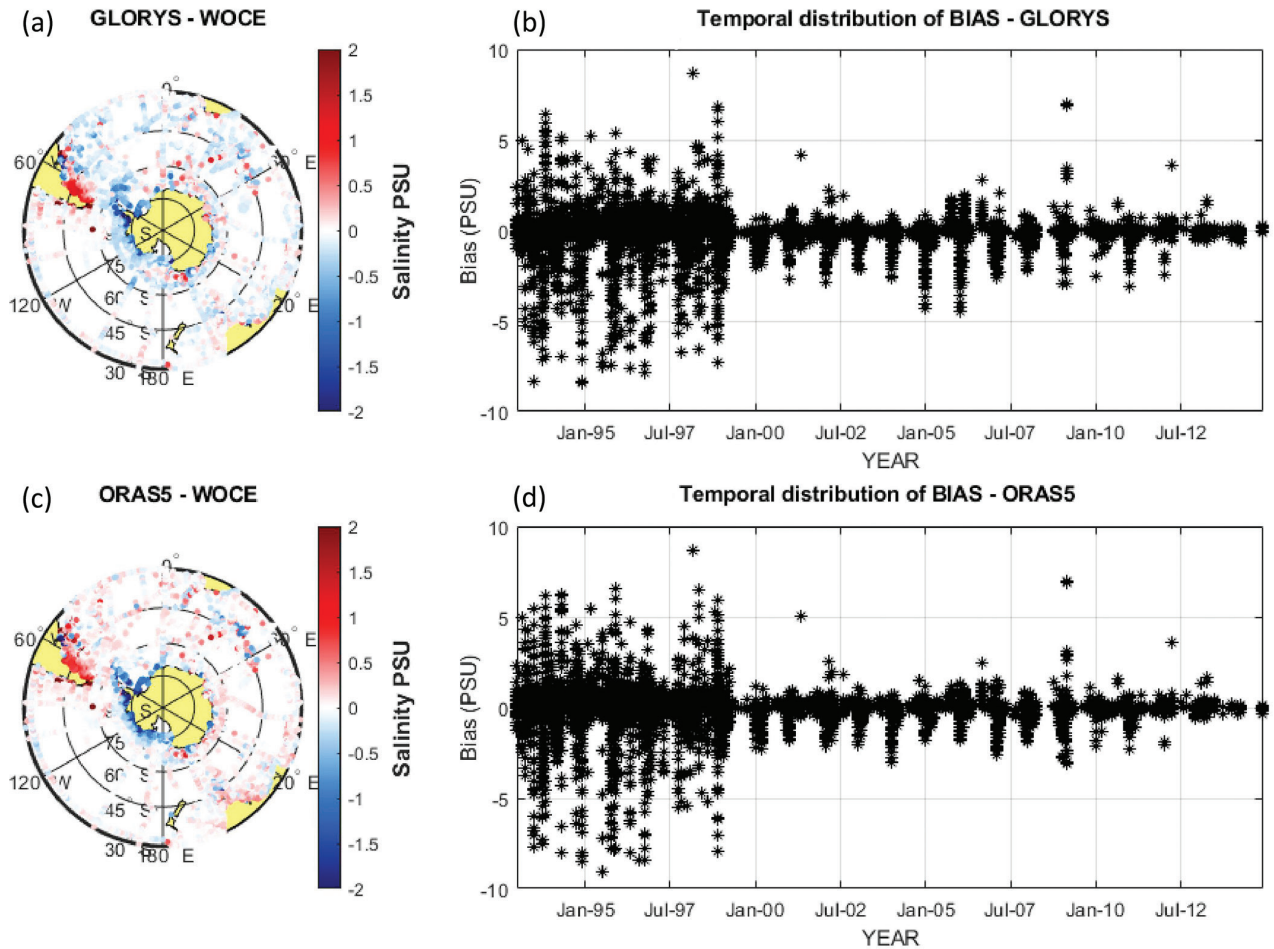


**Fig. 9** Polar map showing the World Ocean Circulation Experiment (WOCE) data collection points along with the differences for salinity between (a) GLORYS2v4 and WOCE, (c) ORAS5 and WOCE (and the temporal distribution of the bias for [b]) GLORYS2v4 and (d) ORAS5. The values in the colour bar are limited to values between -2 and 2 for better visualization.

the Southern Hemisphere were better sampled, as Nicolas & Bromwich (2011) have pointed out regarding atmospheric reanalyses. As shown in the spatial distribution of the differences between the reanalyses and WOCE (Fig. 9a, c), both products present similar patterns and the region with the most prominent differences is coastal South America and the Antarctic Peninsula.

GLORYS2v4 (Fig. 10a) shows positive trends of salinity north of 45° in the SO Atlantic sector, in the Weddell Sea and between New Zealand and Australia. GLORYS2v4 shows an increase in salinity north of 45°, most of the Pacific sector and a decrease between 45° and 60°. The trends presented by GLORYS2v4 are very close to the results found by Aretxabaleta et al. (2015), using the EN4 data set from the Met Office Hadley Centre in the UK (Good et al. 2013) and data from the European Space Agency’s Soil Moisture and Ocean Salinity satellite mission. ORAS5 (Fig. 10b) shows the same significant increase in the Weddell Sea, except for the southern coastal region, which shows a decrease in

salinity, and a slight increase salinity in the region near New Zealand and Australia. Beside these similarities, and the almost identical similar statistical error (RMSE and MAPE), ORAS5 disagrees with the positive sign presented by GLORYS2v4 and found by Aretxabaleta et al. (2015), showing a decrease in salinity in almost all the SO.

To address the question of whether this discrepancy could be caused by the method of entering atmospheric data, we calculated the density fluxes using the equations by Schmitt et al. (1989) in the ERA-Interim data. As expected (since both reanalyses use the same input data from ERA-Interim), the analysis (not shown here) demonstrates that there are no differences between the surface density fluxes; this hypothesis was therefore dismissed. Another hypothesis suggests that the reason for the difference may be the SST nudging process used by ORAS5. The effect of SST nudging on the SSS of ORAS5 is already known as it is shown to generate an increase in the salinity error between 1985 and 2005 (Zuo et al.



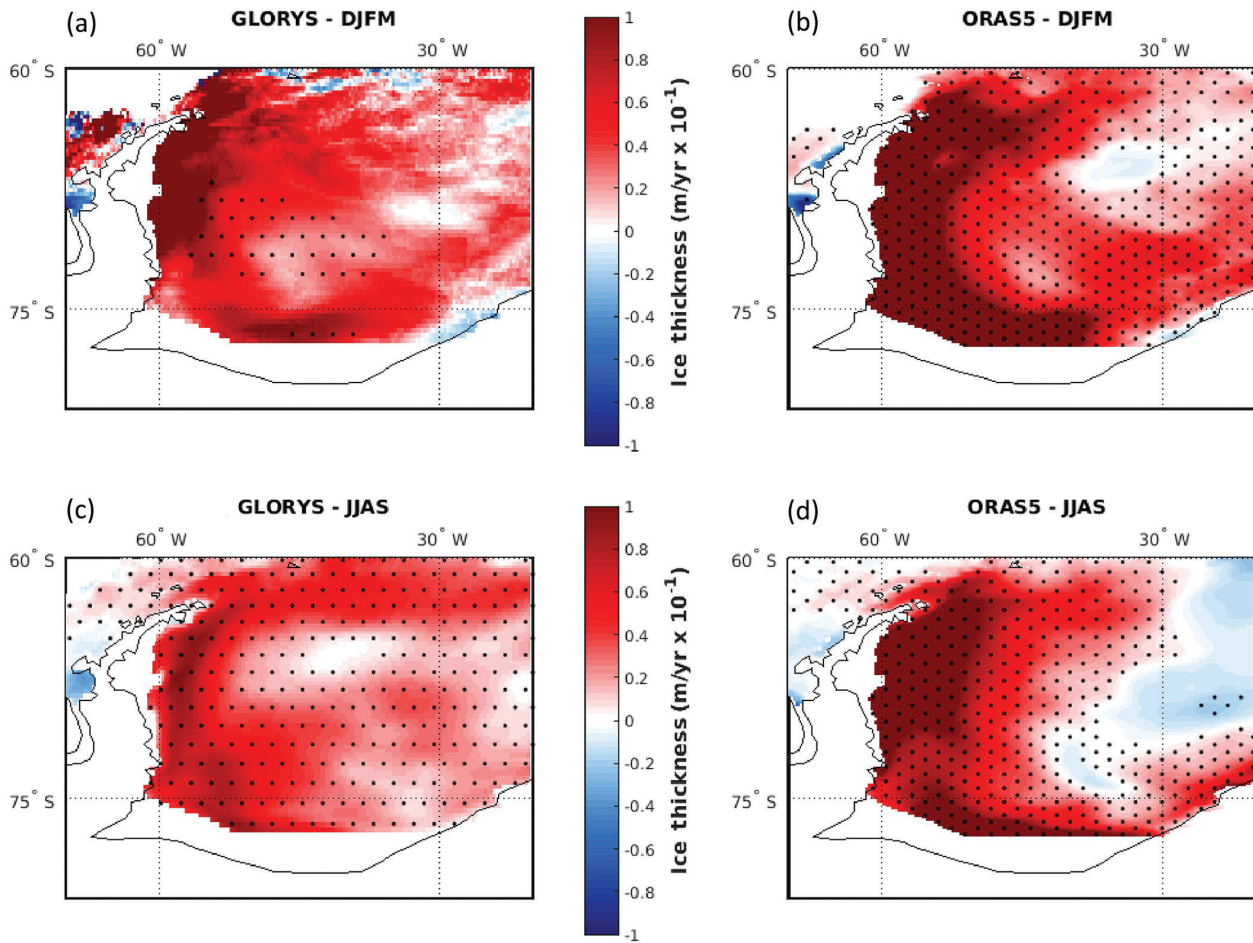


**Fig. 8** Sea-ice thickness in the Weddell Sea for (a, b) austral winter and (c, d) summer, according to (a, c) GLORYS2v4 and (b, d) ORAS5.

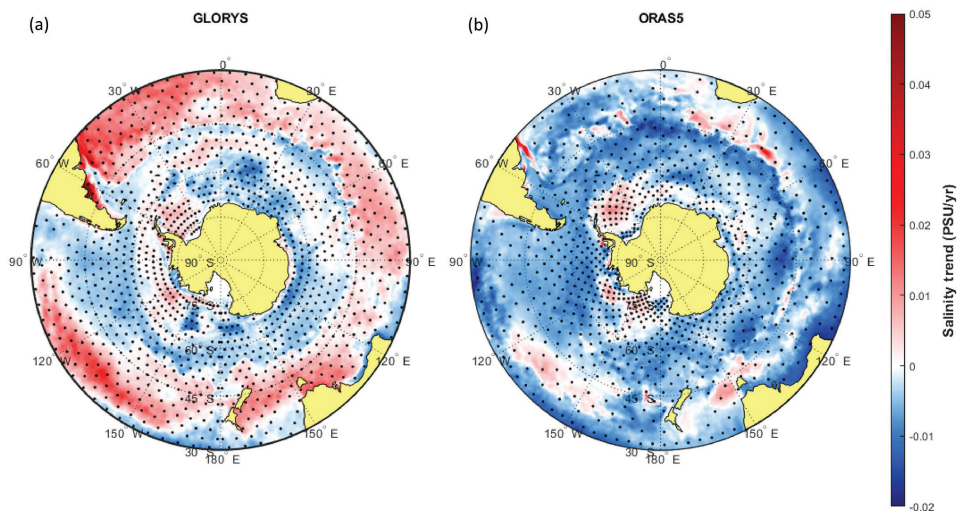


**Fig. 10** Sea-surface salinity (SSS) trends, with points showing regions with trends that are significant at the 95% level for the (a) GLORYS2v4 and (b) ORAS5 reanalyses.

2019). However, Zuo et al. (2019) have shown that, during the Argo Period, that is, 2005–2014, SST nudging causes a reduction in the salinity RMSE in the upper 1000 m in the southern extra-tropics; this nudging accounts for up to 40% of the RMSE reduction in the first 200 m. In fact, the RMSE of ORAS5 relative to the WOCE data is small and close to the values found by GLORYS2v4.

Still, we cannot rule out the hypothesis that SST nudging is the cause of this discrepancy in trends. Using a nudging process like that of ORAS5, Masina & Storto (2017) generated a field of mostly negative trends in the SO. These negative trends are not limited to the surface. Analysing the salinity trend between 0 and 300 m (Supplementary Fig. S1) shows that this error occurs throughout the surface layers. The layer between 300 and 700 m (Supplementary Fig. S1) shows that ORAS5 presents results similar to the trends shown in GLORYS2v4, especially in the Pacific portion of the SO.

## Conclusions

Both reanalyses successfully identify the principal regions of DSW formation, revealing that the reanalyses configurations can be used in the region. Yet there are significant differences between ORAS5 and GLORYS2v4. The difference in the salinity representation by ORAS5 leads to a difference in the surface density, which, in turn, leads to a poor representation of the dense water formation—a key feature of the SO. ORAS5, with its decreasing salinity trend in the Weddell Sea during the austral winter, lacks in production of DSW.

GLORYS2v4 and ORAS5 demonstrate good statistical agreement with WOCE data in the SO, except for the coastal areas. They are also capable of reproducing the climatology patterns of  $\gamma_s^n$ , SST and SSS (not shown here). However, when considering the SSS and the  $\gamma_s^n$  trends, the reanalyses differ in several locations, such as the Weddell Sea. ORAS5 presents negative trends in SSS in most of the SO, which, in turn, lead to a negative trend of  $\gamma_s^n$ . ORAS5 has its SST constrained by nudging to climatology and this seems to be limiting the interpretation of SSS.

A better understanding of salinity trends presents a great challenge for future works and models that are focused on the SO, since even databases collected in situ, such as CORA5 and EN4, present contrasting trends. This is crucial for studying the impacts of climate changes in SSS and how this modifies the Meridional Overturning Circulation and water-mass formation in the SO.

## Acknowledgements

The authors thank the EU Copernicus Marine Service Information, the European Centre for Medium-Range Weather Forecasts, the US National Centers for Environmental Prediction, the Woods Hole Oceanographic Institution and the WOCE database for the data used in this work. They also greatly appreciate the support of the International Center for Theoretical Physics through the Sandwich Training Educational Programme.

## Disclosure statement

The authors report no conflict of interest.

## Funding

The authors gratefully acknowledge the funding support of Coordenação de Aperfeiçoamento de Pessoal de Nível Superior (process no. 88882.437121/2019-01).

## References

- Abernathy R., Cerovecki I., Holland P., Newsom E., Mazloff M. & Talley L. 2016. Water-mass transformation by sea ice in the upper branch of the Southern Ocean overturning. *Nature Geoscience* 9, doi: 10.1038/ngeo2749.
- Akhoudas C.H., Sallée J.-B., Haumann F.A., Meredith M.P., Garabato A.N., Reverdin G., Jullion L., Aloisi G., Benetti M., Leng M.J. & Arrowsmith C. 2021. Ventilation of the abyss in the Atlantic sector of the Southern Ocean. *Scientific Reports* 11, article no. 6760, doi: 10.1038/s41598-021-86043-2.
- Almeida L., Mazloff M.R. & Mata M.M. 2021. The impact of Southern Ocean Ekman pumping, heat and freshwater flux variability on intermediate and mode water export in CMIP models: present and future scenarios. *Journal of Geophysical Research—Oceans* 126, e2021JC017173, doi: 10.1029/2021JC017173.
- Aretxabaleta A.L., Smith K.W. & Ballabrera-Poy J. 2015. Regime changes in global sea surface salinity trend. *Ocean Science Discussions* 12, 983–1011, doi: 10.5194/osd-12-983-2015.
- Azaneu M.V.C., Kerr R., Mata M.M. & Garcia C.A.E. 2013. Trends in the deep Southern Ocean (1958–2010): implications for Antarctic Bottom Water properties and volume export. *Journal of Geophysical Research—Oceans* 118, 4213–4227, doi: 10.1002/jgrc.20303.
- Baines P. & Condie S. 1998. Observations and modelling of Antarctic downslope flows: a review. In S.S. Jacobs & R.F. Weiss (eds.): *Ocean, ice, and atmosphere: interactions at the Antarctic continental margin*. Pp. 29–49. Washington, DC: American Geophysical Union.
- Banks H.T. & Gregory J.M. 2006. Mechanisms of ocean heat uptake in a coupled climate model and the implications for tracer-based predictions of ocean heat uptake. *Geophysical Research Letters* 33, L07608, doi: 10.1029/2005GL025352.

- Barnier B., Madec G., Penduff T., Molines J.-M., Treguier A.-M., Le Sommer J., Beckmann A., Biastoch A., Böning C., Dengg J., Derval C., Durand E., Gulev S., Remy E., Talandier C., Theetten S., Maltrud M., McClean J. & De Cuevas B. 2006. Impact of partial steps and momentum advection schemes in a global ocean circulation model at eddy-permitting resolution. *Ocean Dynamics* 56, 543–567, doi: 10.1007/s10236-006-0082-1.
- Boyer T., Baranova O., Locarnini R., Mishonov A., Grodsky A., Paver C., Weathers K., Smolyar I., Reagan J., Seidov D. & Zweng M. 2019. *World Ocean atlas 2018. Product documentation*. Silver Spring, MD: Ocean Climate Laboratory, National Centers for Environmental Information, National Oceanic and Atmospheric Administration. Doi: 10.13140/RG.2.2.34758.01602.
- Bracegirdle T.J., Shuckburgh E., Sallee J.-B., Wang Z., Meijers A.J.S., Bruneau N., Phillips T. & Wilcox L.J. 2013. Assessment of surface winds over the Atlantic, Indian, and Pacific Ocean sectors of the Southern Ocean in CMIP5 models: historical bias, forcing response, and state dependence. *Journal of Geophysical Research—Atmospheres* 118, 547–562, doi: 10.1002/jgrd.50153.
- Dee D.P., Uppala S.M., Simmons A.J., Berrisford P., Poli P., Kobayashi S., Andrae U., Balmaseda M.A., Balsamo G., Bauer P., Bechtold P., Beljaars A.C.M., van de Berg L., Bidlot J., Bormann N., Delsol C., Dragani R., Fuentes M., Geer A.J., Haimberger L., Healy S.B., Hersbach H., Hólm E.V., Isaksen I., Kållberg P., Köhler M., Matricardi M., McNally A.P., Monge-Sanz B.M., Morcrette J.-J., Park B.-K., Peubey C., de Rosnay P., Tavolato C., Thépaut J.-N. & Vitart F. 2011. The ERA-Interim reanalysis: configuration and performance of the data assimilation system. *Quarterly Journal of the Royal Meteorological Society* 137, 553–597, doi: 10.1002/qj.828.
- Downes S.M., Farneti R., Uotila P., Griffies S.M., Marsland S.J., Bailey D., Behrens E., Bentsen M., Bi D.H., Biastoch A., Böning C., Bozec A., Canuto V.M., Chassignet E., Danabasoglu G., Danilov S., Diansky N., Drange H., Fogli P.G., Gusev A., Howard A., Ilicak M., Jung T., Kelley M., Large W.G., Leboissetier A., Long M., Lu J.H., Masina S., Mishra A., Navarra A., Nurser A.J.G., Patara L., Samuels B.L., Sidorenko D., Spence P., Tsujino H., Wang Q. & Yeager S.G. 2015. An assessment of Southern Ocean water masses and sea ice during 1988–2007 in a suite of interannual CORE-II simulations. *Ocean Modelling* 94, 67–94, doi: 10.1016/j.ocemod.2015.07.022.
- Dufour C.O., Griffies S.M., de Souza G.F., Frenger I., Morrison A.K., Palter J.B., Sarmiento J.L., Galbraith E.D., Dunne J.P., Anderson W.G. & Slater R.D. 2015. Role of mesoscale eddies in cross-frontal transport of heat and biogeochemical tracers in the Southern Ocean. *Journal of Physical Oceanography* 45, 3057–3081, doi: 10.1175/JPO-D-14-0240.1.
- Dunstone N.J. & Smith D.M. 2010. Impact of atmosphere and sub-surface ocean data on decadal climate prediction. *Geophysical Research Letters* 37, L02709, doi: 10.1029/2009GL041609.
- Farneti R., Downes S.M., Griffies S.M., Marsland S.J., Behrens E., Bentsen M., Bi D., Biastoch A., Böning C., Bozec A., Canuto V.M., Chassignet E., Danabasoglu G., Danilov S., Diansky N., Drange H., Fogli P.G., Gusev A., Hallberg R.W., Howard A., Ilicak M., Jung T., Kelley M., Large W.G., Leboissetier A., Long M., Lu J., Masina S., Mishra A., Navarra A., Nurser A.J.G., Patara L., Samuels B.L., Sidorenko D., Tsujino H., Uotila P. & Yeager S.G. 2015. An assessment of Antarctic Circumpolar Current and Southern Ocean Meridional Overturning Circulation during 1958–2007 in a suite of interannual CORE-II simulations. *Ocean Modelling* 93, 84–120, doi: 10.1016/j.ocemod.2015.07.009.
- Ferry N., Parent L., Garric G., Barnier B. & Jourdain N. 2010. Mercator global eddy permitting ocean reanalysis GLORYS1V1: description and results. *Mercator Quarterly Newsletter* 36 (January), 15–27.
- Foldvik A., Gammelsrød T., Østerhus S., Fahrback E., Rohardt G., Schröder M., Nicholls K.W., Padman L. & Woodgate R.A. 2004. Ice shelf water overflow and bottom water formation in the southern Weddell Sea. *Journal of Geophysical Research—Oceans* 109, C02015, doi: 10.1029/2003JC002008.
- Foster T.D. 1995. Abyssal water mass formation off the eastern Wilkes Land coast of Antarctica. *Deep-Sea Research Part I* 42, 501–522, doi: 10.1016/0967-0637(95)00002-N.
- Foster T.D. & Carmack E.C. 1976. Frontal zone mixing and Antarctic Bottom Water formation in the southern Weddell Sea. *Deep Sea Research and Oceanographic Abstracts* 23, 301–317, doi: 10.1016/0011-7471(76)90872-X.
- Frölicher T.L., Sarmiento J.L., Paynter D.J., Dunne J.P., Krasting J.P. & Winton M. 2015. Dominance of the Southern Ocean in anthropogenic Carbon and heat uptake in CMIP5 models. *Journal of Climate* 28, 862–886, doi: 10.1175/JCLI-D-14-00117.1.
- Good S.A., Martin M.J. & Rayner N.A. 2013. EN4: quality controlled ocean temperature and salinity profiles and monthly objective analyses with uncertainty estimates. *Journal of Geophysical Research—Oceans* 118, 6704–6716, doi: 10.1002/2013JC009067.
- Gordon A., Zambianchi E., Orsi A., Visbeck M., Giulivi C., Whitworth T. & Spezie G. 2004. Energetic plumes over the western Ross Sea continental slope. *Geophysical Research Letters* 31, L21302, doi: 10.1029/2004GL020785.
- Gordon A.L. 2001. Bottom water formation. In J.H. Steele (ed.): *Encyclopedia of ocean sciences*. 2nd edn. Pp. 415–421. Oxford: Academic Press.
- Gordon A.L., Huber B.A., Hellmer H.H. & Field A. 1993. Deep and Bottom Water of the Weddell Sea's western rim. *Science* 262, 95–97, doi: 10.1126/science.262.5130.95.
- Gordon A.L., Orsi A.H., Muench R., Huber B.A., Zambianchi E. & Visbeck M. 2009. Western Ross Sea continental slope gravity currents. *Deep-Sea Research Part II* 56, 796–817, doi: 10.1016/j.dsr2.2008.10.037.
- Hartin C.A., Fine R.A., Sloyan B.M., Talley L.D., Chereskin T.K. & Happell J. 2011. Formation rates of Subantarctic Mode Water and Antarctic Intermediate Water within the South Pacific. *Deep-Sea Research Part I* 58, 524–534, doi: 10.1016/j.dsr.2011.02.010.
- Jackett D.R. & McDougall T.J. 1997. A neutral density variable for the world's oceans. *Journal of Physical Oceanography* 27, 237–263, doi: 10.1175/1520-0485(1997)027<0237:ANDVFT>2.0.CO;2.



- Jacobs S.S., Amos A.F. & Bruchhausen P.M. 1970. Ross Sea oceanography and Antarctic Bottom Water formation. *Deep Sea Research and Oceanographic Abstracts* 17, 935–962, doi: 10.1016/0011-7471(70)90046-X.
- Johnson G.C. 2008. Quantifying Antarctic Bottom Water and North Atlantic Deep Water volumes. *Journal of Geophysical Research—Oceans* 113, C05027, doi: 10.1029/2007JC004477.
- Justino F., Setzer A., Bracegirdle T., Mendes D., Grimm A., Dechiche G. & Schaefer C. 2011. Harmonic analysis of climatological temperature over Antarctica: present day and greenhouse warming perspectives. *International Journal of Climatology* 31, 514–530, doi: 10.1002/joc.2090.
- Justino F., Silva A.S., Pereira M.P., Stordal F., Lindemann D. & Kucharski F. 2015. The large-scale climate in response to the retreat of the West Antarctic Ice Sheet. *Journal of Climate* 28, 637–650, doi: 10.1175/JCLI-D-14-00284.1.
- Khatiwala S., Tanhua T., Mikaloff F.S., Gerber M., Doney S.C., Graven H.D., Gruber N., McKinley G.A., Murata A., Ríos A.F. & Sabine C.L. 2013. Global Ocean storage of anthropogenic carbon. *Biogeosciences* 10, 2169–2191, doi: 10.5194/bg-10-2169-2013.
- Lumpkin R. & Speer K. 2007. Global ocean meridional overturning. *Journal of Physical Oceanography* 37, 2550–2562, doi: 10.1175/JPO3130.1.
- Marinov I., Gnanadesikan A., Toggweiler J.R. & Sarmiento J.L. 2006. The Southern Ocean biogeochemical divide. *Nature* 441, 964–967, doi: 10.1038/nature04883.
- Marshall J., Scott J.R., Armour K.C., Campin J.-M., Kelley M. & Romanou A. 2015. The ocean's role in the transient response of climate to abrupt greenhouse gas forcing. *Climate Dynamics* 44, 2287–2299, doi: 10.1007/s00382-014-2308-0.
- Marshall J. & Speer K. 2012. Closure of the Meridional Overturning Circulation through Southern Ocean upwelling. *Nature Geoscience* 5, 171–180, doi: 10.1038/ngeo1391.
- Masina S. & Storto A. 2017. Reconstructing the recent past ocean variability: status and perspective. *Journal of Marine Research* 75, 727–764, doi: 10.1357/002224017823523973.
- Moorman R., Morrison A.K. & McC. Hogg A. 2020. Thermal responses to Antarctic ice shelf melt in an eddy-rich global ocean–sea ice model. *Journal of Climate* 33, 6599–6620, doi: 10.1175/JCLI-D-19-0846.1.
- Nicolas J. & Bromwich D. 2011. Precipitation changes in high southern latitudes from global reanalyses: a cautionary tale. *Surveys in Geophysics* 32, 475–494, doi: 10.1007/s10712-011-9114-6.
- Ohshima K.I., Fukamachi Y., Williams G.D., Nihashi S., Roquet F., Kitade Y., Tamura T., Hirano D., Herraiz-Borreguero L., Field I., Hindell M., Aoki S. & Wakatsuchi M. 2013. Antarctic Bottom Water production by intense sea-ice formation in the Cape Darnley polynya. *Nature Geoscience* 6, 235–240, doi: 10.1038/ngeo1738.
- Orsi A.H., Johnson G.C. & Bullister J.L. 1999. Circulation, mixing, and production of Antarctic Bottom Water. *Progress in Oceanography* 43, 55–109, doi: 10.1016/S0079-6611(99)00004-X.
- Pellichero V., Sallée J.-B., Chapman C.C. & Downes S.M. 2018. The Southern Ocean meridional overturning in the sea-ice sector is driven by freshwater fluxes. *Nature Communications* 9, article no. 1789, doi: 10.1038/s41467-018-04101-2.
- Rintoul S.R. 1998. On the origin and influence of Adélie Land Bottom Water. In S.S. Jacobs & R.F. Weiss (eds.): *Ocean, ice, and atmosphere: interactions at the Antarctic continental margin*. Pp. 151–171. Washington, DC: American Geophysical Union.
- Rintoul S.R. 2007. Rapid freshening of Antarctic Bottom Water formed in the Indian and Pacific oceans. *Geophysical Research Letters* 34, L06606, doi: 10.1029/2006GL028550l.
- Rintoul S.R. 2018. The global influence of localized dynamics in the Southern Ocean. *Nature* 558, 209–218, doi: 10.1038/s41586-018-0182-3.
- Sabine C.L., Feely R.A., Gruber N., Key R.M., Lee K., Bullister J.L., Wanninkhof R., Wong C.S., Wallace D.W.R., Tilbrook B., Millero F.J., Peng T.-H., Kozyr A., Ono T. & Ríos A.F. 2004. The Oceanic sink for anthropogenic CO<sub>2</sub>. *Science* 305, 367–371, doi: 10.1126/science.1097403.
- Sallée J.-B., Shuckburgh E., Bruneau N., Meijers A.J.S., Bracegirdle T.J., Wang Z. & Roy T. 2013. Assessment of Southern Ocean water mass circulation and characteristics in CMIP5 models: historical bias and forcing response. *Journal of Geophysical Research—Oceans* 118, 1830–1844, doi: 10.1002/jgrc.20135.
- Sarmiento J.L., Gruber N., Brzezinski M.A. & Dunne J.P. 2004. High-latitude controls of thermocline nutrients and low latitude biological productivity. *Nature* 427, 56–60, doi: 10.1038/nature02127.
- Schmitt R., Bogden P. & Dorman C. 1989. Evaporation minus precipitation and density fluxes for the North Atlantic. *Journal of Physical Oceanography* 19, 1208–1221, doi: 10.1175/1520-0485(1989)019<1208:EMPADF>2.0.CO;2.
- Schneider D.P. & Reusch D.B. 2016. Antarctic and Southern Ocean surface temperatures in CMIP5 models in the context of the surface energy budget. *Journal of Climate* 29, 1689–1716, doi: 10.1175/JCLI-D-15-0429.1.
- Servonnat J., Mignot J., Guilyardi E., Swingedouw D., Séférian R. & Labetoulle S. 2014. Reconstructing the sub-surface ocean decadal variability using surface nudging in a perfect model framework. *Climate Dynamics* 44, 315–338, doi: 10.1007/s00382-014-2184-7.
- Sigman D.M. & Boyle E.A. 2000. Glacial/interglacial variations in atmospheric carbon dioxide. *Nature* 407, 859–869, doi: 10.1038/35038000.
- Silvano A. 2020. Changes in the Southern Ocean. *Nature Geoscience* 13, 4–5, doi: 10.1038/s41561-019-0516-2.
- Sloyan B.M. & Rintoul S.R. 2001. The Southern Ocean limb of the global deep overturning circulation. *Journal of Physical Oceanography* 31, 143–173, doi: 10.1175/1520-0485(2001)031<0143:TSOLOT>2.0.CO;2.
- Talley L.D., Pickard G.L., Emery W.J. & Swift J.H. 2011. *Descriptive physical oceanography: an introduction*. 6th edn. Boston, MA: Elsevier.
- Tamura T., Ohshima K.I. & Nihashi S. 2008. Mapping of sea ice production for Antarctic coastal polynyas. *Geophysical Research Letters* 35, L07606, doi: 10.1029/2007GL032903.
- Uppala S.S., Dee D., Kobayashi S. & Simmons A. 2008. Evolution of reanalysis at ECMWF. Unpublished ms.



- Wang G., Cheng L., Abraham J. & Chongyin L. 2018. Consensuses and discrepancies of basin-scale ocean heat content changes in different ocean analyses. *Climate Dynamics* 50, 2471–2487, doi: 10.1007/s00382-017-3751-5.
- Wang G. & Dommenget D. 2015. The leading modes of decadal SST variability in the Southern Ocean in CMIP5 simulations. *Climate Dynamics* 47, 1775–1792, doi: 10.1007/s00382-015-2932-3.
- Watson A.J. & Naveira Garabato A.C. 2006. The role of Southern Ocean mixing and upwelling in glacial–interglacial atmospheric CO<sub>2</sub> change. *Tellus B* 58, 73–87, doi: 10.1111/j.1600-0889.2005.00167.x.
- Williams G., Aoki S., Jacobs S., Rintoul S., Tamura T. & Bindoff N. 2010. Antarctic Bottom Water from the Adélie and George V Land Coast, East Antarctica (140–149°E). *Journal of Geophysical Research—Oceans* 115, doi: 10.1029/2009JC005812.
- Williams G.D., Herraiz-Borreguero L., Roquet F., Tamura T., Ohshima K.I., Fukamachi Y., Fraser A.D., Gao L., Chen H., McMahon C.R., Harcourt R. & Hindell M. 2016. The suppression of Antarctic bottom water formation by melting ice shelves in Prydz Bay. *Nature Communications* 7, article no. 12577, doi: 10.1038/ncomms12577.
- Yamamoto A., Abe-Ouchi, A., Shigemitsu M., Oka A., Takahashi K., Ohgaito R. & Yamanaka Y. 2015. Global deep ocean oxygenation by enhanced ventilation in the Southern Ocean under long-term global warming. *Global Biogeochemical Cycles* 29, 1801–1815, doi: 10.1002/2015GB005181.
- Zuo H., Balmaseda M.A., Tietsche S., Mogensen K. & Mayer M. 2019. The ECMWF operational ensemble reanalysis–analysis system for ocean and sea ice: a description of the system and assessment. *Ocean Science* 15, 779–808, doi: 10.5194/os-15-779-2019.